ELSEVIER

Journal of Molecular Catalysis A: Chemical 155 (2000) 131–142

JOURNAL OF MOLECULAR CATALYSIS A: CHEMICAL

www.elsevier.com/locate/molcata

Pillaring and photocatalytic property of partially substituted layered titanates, $Na_2Ti_{3-x}M_xO_7$ and $K_2Ti_{4-x}M_xO_9$ (M = Mn, Fe, Co, Ni, Cu)

Masato Machida *, Xu Wei Ma, Hideki Taniguchi, Jun-ichi Yabunaka, Tsuyoshi Kijima

Department of Materials Science, Faculty of Engineering, Miyazaki University, 1-1 Gakuen Kibanadai Nishi, Miyazaki 889-2192, Japan

Received 1 October 1998; accepted 1 February 1999

Abstract

Porous pillared materials have been synthesized from substituted tri- and tetratitanates ($Na_2Ti_{3-x}M_xO_7$, $K_2Ti_{4-x}M_xO_9$, M = Mn, Fe, Co, Ni, Cu, $x \leq 0.3$) by a stepwise exchange process. The microstructure of pillared samples was characterized by a number of cleavages running parallel with TiO_6 layers, which produced a waffle-like texture. The pillared samples showed 10–25 times larger BET surface areas (50–120 m^2/g) as compared to pristine samples. The photocatalytic activity of 1 wt.% Pt/titanates for H_2 evolution from CH_3OH/H_2O mixtures was enhanced by pillaring in accord with an increase of the surface area. Partial substitution of various transition elements for the Ti site significantly affected the H_2 evolution rate.

Keywords: Layered titanate; Pillared structure; Intercalation; Photocatalysis

1. Introduction

The synthesis of pillared structures from layered materials has led to the development of a new class of porous catalysts [1]. Pillared layered materials are prepared by intercalation of large polymeric inorganic cations or metal alkoxides into layered hosts, which are converted to oxide pillars after calcination. The resulting microporous structure is characterized by interlayer spacings of ca. 1 nm and high specific surface areas. Another interesting feature of pillared materials is a wide variety of possible chemical combinations between layers and pillars. Apart from the conventional clays and related materials, several researchers have recently reported the pillaring of layered transition metal oxides, such as titanates and niobates [2–9]. Their catalytic and electronic properties are expected to lead to a novel family of functional porous solids. Actually, it has been already reported by Domen et al. [7,10] and Sato et al. [11] that pillared materials prepared from layered niobates exhibit the excellent photocatalytic activity for hydrogen evolution reactions. In this study, we have synthesized pillared

* Corresponding author. Tel.: +81-985-58-7312; fax: +81-985-58-7323.

E-mail address: machida@material.chem.miyazaki-u.ac.jp (M. Machida).

1381-1169/00/$ - see front matter
PII: S1381-1169(99)00329-5

structure from two different types of layered titanates which are partially substituted by various transition elements. An attempt was made to evaluate the effect of pillaring and partial substitution on the crystal structure, microstructure, and photocatalytic property.

2. Experimental

2.1. Sample preparation

Sodium trititanate, potassium tetratitanate, and their substituted samples ($Na_2Ti_{3-x}M_xO_7$, $K_2Ti_{4-x}M_xO_9$, M = Mn, Fe, Co, Ni, Cu, x = 0.15–0.30) were prepared by calcining mixtures of carbonate (Na_2CO_3 or K_2CO_3) and oxide (TiO_2 and other transition metal oxides) powders at 800°C for 30 h. The pillared samples were prepared by a stepwise exchange process [2–9]. In the first step, the samples (3.0 g) were exchanged in 1 mol/l HCl (200 ml) at room temperature for 1 week to give protonated derivatives. Intercalation of hexylamine was carried out by mixing the protonated sample (1.0 g) in an aqueous solution of 5 mol/l *n*-$C_6H_{13}NH_2$ at room temperature for 1 week. The solid product was then treated with pillaring agents, tetraethyl orthosilicate (TEOS) or aqueous solution of aluminum hydroxide oligomers, $[Al_{13}O_4(OH)_{24}(H_2O)_{12}]^{7+}$ (Al_{13}), at 60°C for 3 days. The Al_{13} solution was prepared by slowly adding $C_6H_{13}NH_2$ to $AlCl_3$ to obtain a final hydrolysis ratio, OH/Al = 2.3 (pH = 4.0–4.5), and following aging at 60°C for 4 h. After reaction with these pillaring agents, the resultant solid product was centrifuged, washed with water or ethanol and air-dried at room temperature. The porous pillared samples were obtained by calcination at elevated temperatures (300°C–500°C) in a stream of O_2.

2.2. Characterization and photocatalytic reaction

The crystal structure of as prepared samples was identified by using a powder X-ray diffractometer (XRD, Shimadzu XD-D1) equipped with Cu-Kα radiation (30 kV, 20 mA) and a monochromater. An infrared spectrometer (Jasco FT-IR-300) was used for the chemical structure analysis. Chemical composition of samples was determined by energy-dispersive X-ray analysis (EDS, Horiba) and atomic absorption (Hitachi Z8000). Thermal gravimetric (TG) analysis of as prepared samples was carried out by using an ULVAC TGD-5000 at a heating rate of 10°C/min in air. The BET surface area and pore size distribution were obtained by measuring N_2 adsorption isotherms at 77 K. The microstructure of samples was observed by FE-SEM (Hitachi 4100) and TEM (JEOL 2000FX). Diffuse reflectance spectra were recorded with a UV–vis spectrometer (Jasco V-550).

The photocatalytic H_2 evolution from aqueous solution of 4 mol/l CH_3OH was conducted in an inner irradiation Pyrex cell, which is connected to a conventional gas circulation system, under irradiation with light from a 400 W high-pressure Hg lamp. The powder sample (0.2 g) before and after photodeposition of platinum (1 wt.%) was suspended in the solution and stirred during irradiation. Prior to the reaction, the system was evacuated to remove air and then purged with 150 mmHg of Ar. The amount of H_2 evolved was determined by using an on-line gas chromatograph (GL Science 370, TCD, Ar carrier) with MS-5A and Porapak-Q columns as well as a quadrupole mass spectrometer (Spectra Metrics, Monitor).

3. Results and discussion

3.1. Crystal structure and chemical composition in stepwise exchange process

X-ray diffraction patterns of tri- and tetratitanates ($NaTi_3O_7$ and $K_2Ti_4O_9$) were respectively in good agreement with the data already reported [12]. The crystal structure of these titanates is built up from a unit of three or four TiO_6 octahedra arranged in a line by edge shar-

ing (see Fig. 6c). These units are joined to similar blocks above and below to form zigzag strings. The strings are combined by sharing corners of octahedra to form staggered sheets. We have found that the Ti^{4+} site in this sheet could be partially replaced by various transition metals (Mn, Fe, Co, Ni, and Cu) without structural deterioration up to $x = 0.3$ for $Na_2Ti_{3-x}M_xO_7$ and $x = 0.2$ for $K_2Ti_{4-x}M_xO_9$.

The structural change of the layered titanates during stepwise exchange to pillared derivatives was studied by XRD. Fig. 1 shows representative diffraction patterns for the $Na_2Ti_{2.7}Mn_{0.3}O_7$ system. The stepwise exchange could be observed as a shift of the (100) reflection at $2\theta = 10.6°$, which corresponds to the interlayer distance ($d = 0.83$ nm) between two adjacent TiO_6 sheets. After protonation in 1 mol/l HCl the interlayer distance decreased from 0.83 to 0.78 nm. Since the TG analysis indicated that the interlayer of pristine and protonated samples was not hydrated, the observed decrease in the interlayer distance results from different size of interlayer cations. The interlayer distance was then significantly expanded to 2.1 nm ($2\theta = 4.2°$) by following intercalation of $C_6H_{13}NH_2$. The corresponding interlayer spacing of ca. 1.5 nm is much lager than the chain length of *n*-hexylammonium ions (ca. 1.0 nm), suggesting the bilayer configuration of alkyl chains as was pointed out by Hou et al. [8]. Mixing the hexylamine-intercalated sample with TEOS led to little change of the interlayer distance, but the EDS analysis clearly showed that TEOS was absorbed into the organophilic interlayer region. After calcination at 400°C in air, FT-IR measurement revealed the complete elimination of the organic components (ν_{CH} 2840–3960 cm^{-1}, δ_{NH} 1450–1520 cm^{-1}) and formation of a Si–O network (ν_{SiO} 1000–1100 cm^{-1}). The resultant pillared titanate possessed an interlayer distance of 1.6 nm ($2\theta = 5.6°$), which corresponds to the interlayer spacing of ca. 1.0 nm between adjacent TiO_6 sheets. However, a substantial broadening and loss of the peak intensity of the (100) reflection suggest the lack of regularity of the layer stacking. Other SiO_2- or Al_2O_3-pillared samples could be also prepared from layered

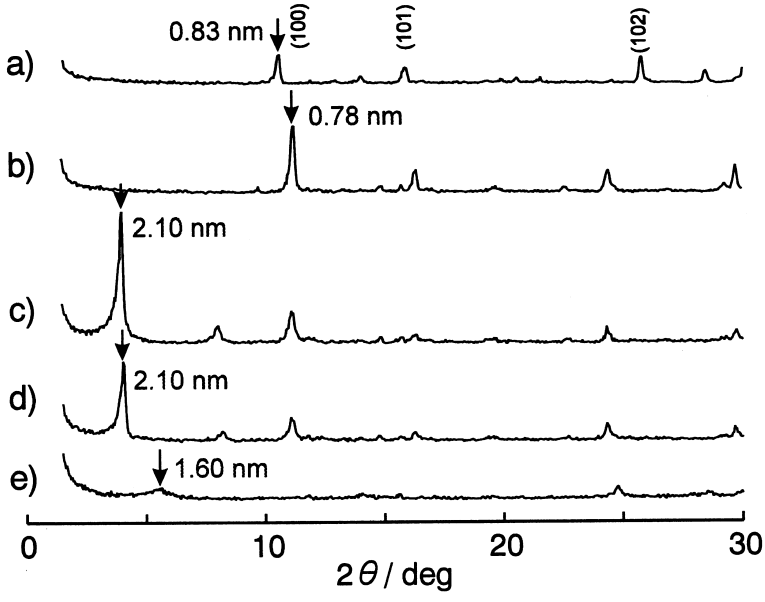

Fig. 1. XRD patterns of $Na_2Ti_{2.7}Mn_{0.3}O_7$. (a) Pristine sample, (b) after protonation, (c) after intercalation of hexylamine, (d) after intercalation of TEOS, and (e) (d) calcined at 400°C in air.

titanates and their substituted derivatives in the same manner.

Table 1 summarizes the results of chemical composition analysis for $Na_2Ti_{3-x}M_xO_7$ in the stepwise exchange process. After more than 95 at.% of sodium ion was extracted during protonation in 1 mol/l HCl, part of substituted transition elements was eluted from the solid. Their residual amounts were quite different, e.g., 86 at.% of Mn remained whereas 78 at.% of Cu dissolved out for the nominal composition of $x = 0.3$. As a result of this considerable elution, the pillared structure of Cu-substituted samples was easily collapsed upon heating. The uptake of hexylamine by protonated samples was determined by TG measurement, which showed the weight loss caused by elimination of hexylamine at 400°C–550°C. The substitution for Ti resulted in the increased uptake except the Cu case ($x = 0.3$). The amount of TEOS incorporated into the layered titanate as a pillaring agent was also dependent on the substituted transition element, increasing in accord with the uptake of hexylamine. Therefore, formation of hexylamine bilayers in the interlayer is effective in promoting the incorporation of TEOS.

3.2. Microstructure of pillared layered titanates

Fig. 2 showed the BET surface area of unsubstituted tri- and tetratitanates. The pristine powders of these two types of titanates showed low surface areas less than 5 m^2/g, which were little changed after protonation. In contrast, the pillared titanates showed much larger surface areas above 50 m^2/g. From XRD measurement, the pillared structure was thermostable up to 500°C, but the surface areas showed their maximum at 400°C. Fig. 3 shows the surface area of SiO_2-pillared $Ti_{3-x}M_xO_7$ after calcination at 400°C. The surface area increased after the substitution and the largest value of 120 m^2/g was attained for $M = Mn$ ($x = 0.3$). It should be noted that the surface area is roughly dependent on the SiO_2 content shown in Table 1. This result suggests that higher density of SiO_2 pillaring is effective in producing large surface areas after calcination. Among the substituted pillared titanates, Cu-substituted sample showed the lowest surface areas because of the structural collapse caused by the elution of Cu ions in the protonation step. Fig. 4 shows the typical pore size distribution calculated from N_2 ad-

Table 1
Chemical composition in stepwise exchange processes of $NaTi_{3-x}M_xO_7$

M	x[a]	Protonation[b] (at.%)	Residual[c] M (at.%)	Uptake of amine (mol/mol)	Uptake of TEOS (mol/mol)
Ti	–	95.5	–	0.12	0.26
Mn	0.15	98.2	85.1	0.17	0.43
	0.30	97.4	86.1	0.38	0.70
Fe	0.15	96.8	73.8	0.12	0.39
	0.30	95.4	67.8	0.12	0.40
Co	0.15	98.7	77.7	0.18	0.39
	0.30	95.3	72.2	0.15	0.38
Ni	0.15	96.4	69.4	0.21	0.51
	0.30	95.4	80.5	0.20	0.54
Cu	0.15	95.8	5.2	0.13	0.29
	0.30	97.2	21.6	0.01	0.10

[a] Nominal composition.
[b] $H/(H + Na) \times 100$.
[c] Residual M after protonation in HCl solution.

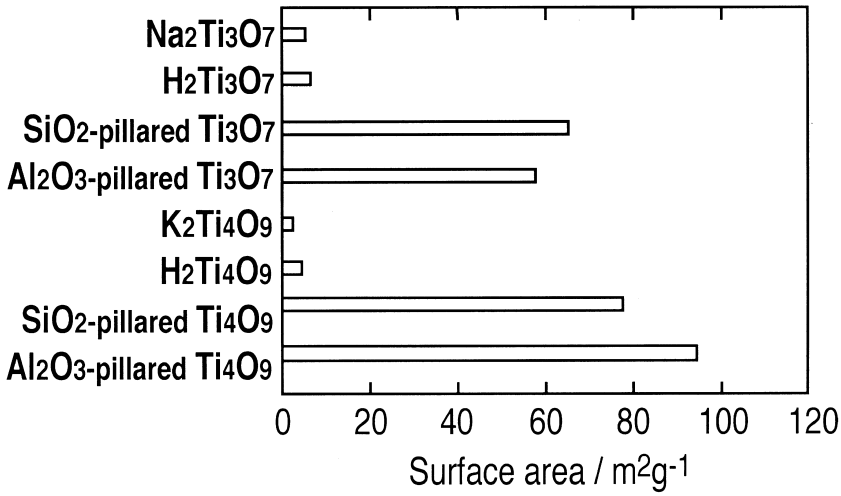

Fig. 2. BET surface areas of ion-exchanged and pillared layered titanates. Pillared samples were calcined at 400°C.

sorption isotherms at 77 K. The pillared titanates showed a peak centered at ca. 3 nm, which was absent in the pristine sample. The disagreement between the pore size and interlayer spacing (ca. 1 nm) estimated from XRD arises from inhomogeneity of the pillared structure as described below.

The microstructure of tetratitanate samples before and after SiO_2-pillaring was observed by SEM as shown in Fig. 5. The pristine powders ($K_2Ti_4O_9$) consisted of planar or columnar microcrystals of 0.5–2 μm long and 0.1–0.4 μm wide. These well-developed microcrystals possessed smooth surface, of which geometrical area is close to the BET surface area. After pillaring and calcination at 400°C several microcrystals were deformed and cracked, but no significant change was observed in their particles size. Since the deposition of amorphous SiO_2 particles on the microcrystals was negligible, the increased surface area of pillared samples (Fig. 2) is considered due to the formation of intraparticle pores accessible by N_2 molecules.

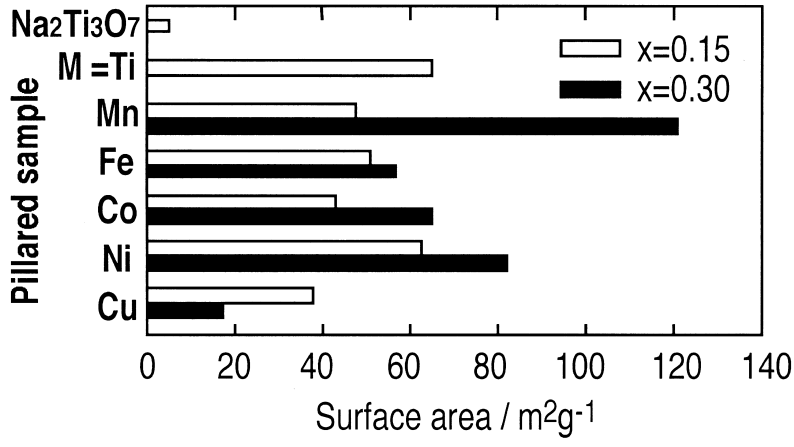

Fig. 3. BET surface areas of SiO_2-pillared $Ti_{3-x}M_xO_7$ after calcination at 400°C.

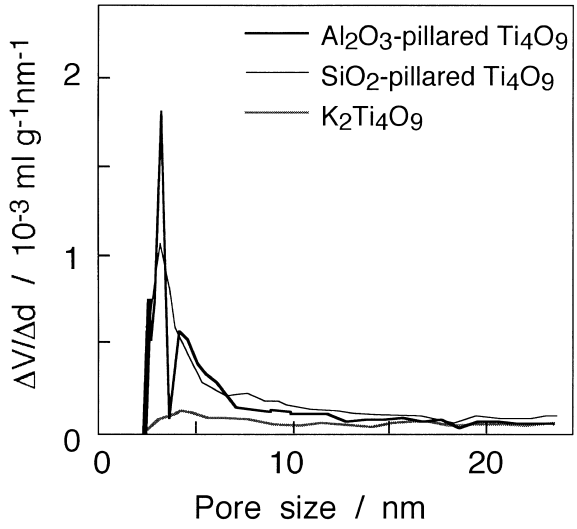

Fig. 4. Pore size distribution of pillared layered titanates after calcination at 400°C.

Fig. 6a shows a TEM photograph of pristine $K_2Ti_4O_9$ particles. Selected area electron diffraction (SAD) with an incident beam normal to the prism plane of several different crystals showed a single-crystal pattern (Fig. 6b) consistent with the monoclinic lattice of $K_2Ti_4O_9$ (Fig. 6c), which is composed of TiO_6 octahedra sheets stacking along the a^* direction. Since all

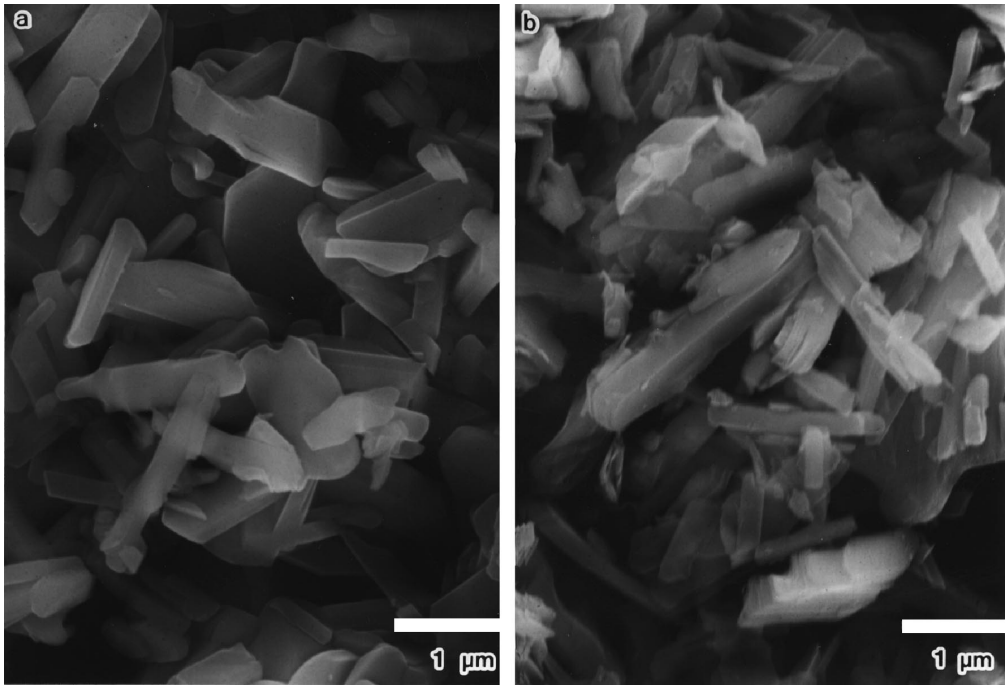

Fig. 5. SEM photographs of (a) $K_2Ti_4O_9$ and (b) SiO_2-pillared tetratitanate after calcination at 400°C.

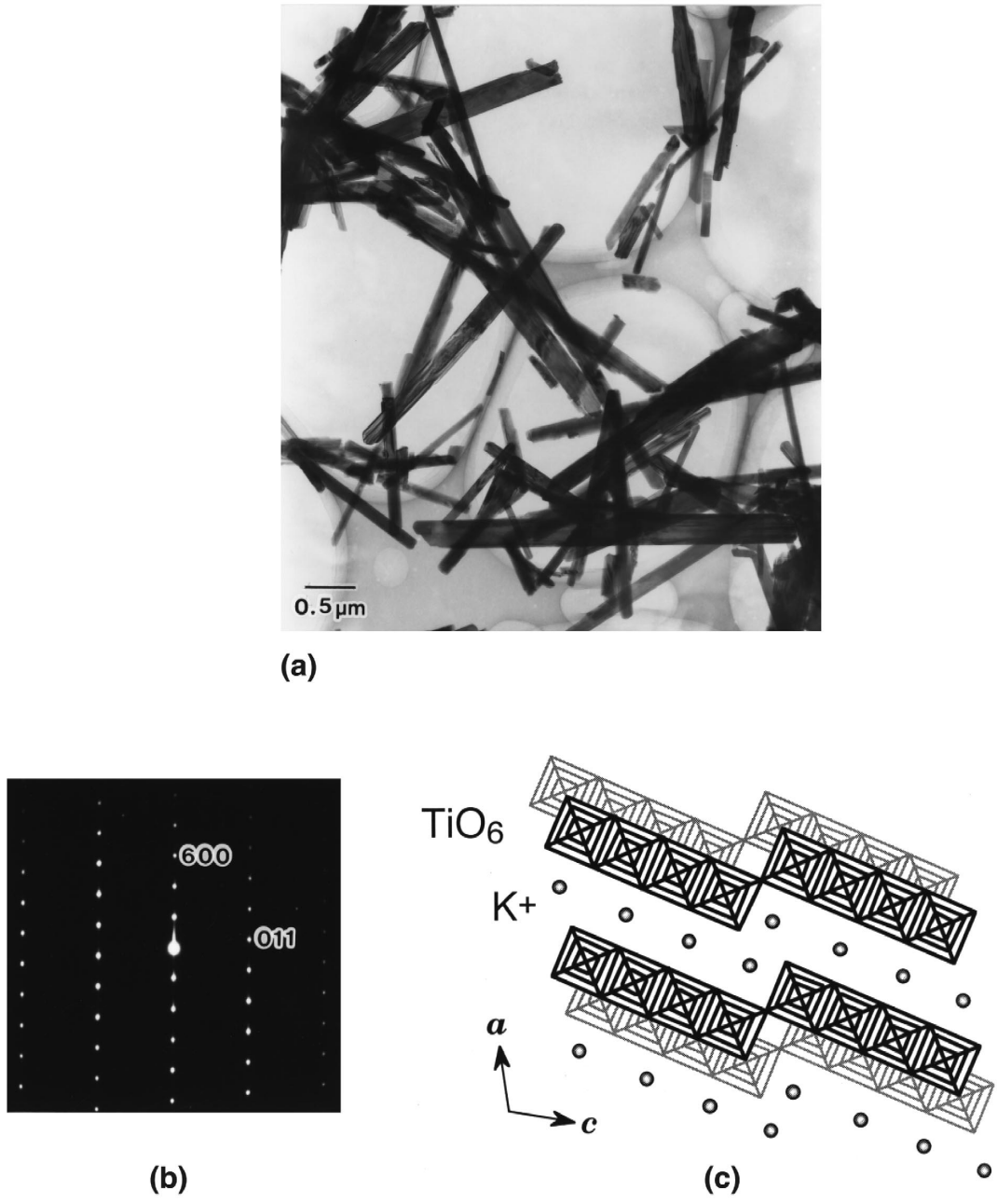

Fig. 6. (a) TEM images, (b) selected area diffraction patterns of $K_2Ti_4O_9$, and (c) crystal structure of $K_2Ti_4O_9$ projected on (010).

the diffraction spots can be indexed with the [0$\bar{1}$1] zone axis, it was demonstrated that the direction of layer-stacking is just perpendicular to the fiber axis of microcrystals. Fig. 7 shows the image of SiO_2-pillared tetratitanate samples after calcination at 400°C. In contrast to the pristine microcrystals, these particles were characterized by many cleavages running parallel with the TiO_6 sheets in the vicinity of tale end surface (Fig. 7a). This texture is consistent with

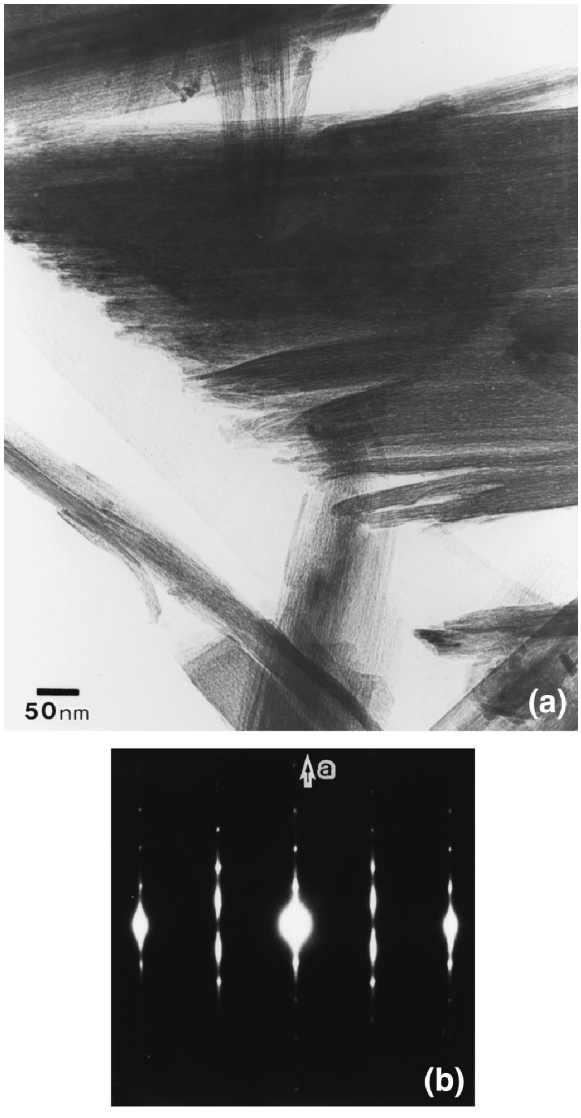

Fig. 7. (a) TEM images and (b) selected area diffraction patterns of SiO_2-pillared tetratitanate after calcination at 400°C.

the formation of nano-spaces separated by the oxide pillars between layers. Oxide pillars could be observed as an amorphous contrast between layers but negligibly on the outer surface of the particles. In the SAD patterns with the $[0\bar{1}1]$ zone axis (Fig. 7b), all diffraction spots were elongated along the a^* direction, indicating lack of the periodicity of layer stacking. Actually, many cleavages with different spacings as well as interlayers remaining unpillared could be observed. How to complete the pillaring reactions without structural deterioration is the key to the improvement of the surface area and pore size distribution. We have also conducted TEM observation on Al_2O_3-pillared samples obtained from tri- and tetratitanates as well, but their microstructure was scarcely influenced by the difference of pillaring agents.

3.3. Photocatalytic property of pillared titanates

Fig. 8a shows the UV–vis diffuse reflectance spectra of pristine, protonated, and SiO_2-pillared trititanates together with their band gap energy. The absorption onset of $Na_2Ti_3O_7$ was shifted to longer wavelength after the protonation and subsequent pillaring processes. This corresponds to the band gap energy decreasing from 3.59 to 3.18 eV. Since the similar behavior was also observed for the $K_2Ti_4O_9$ system, the band-gap transition of layered titanates seems sensitive to the interlayer spacing or interlayer species. The substituted titanates showed no clear-cut absorption edges because of absorptions in the visible light region, which is associated with the presence of impurity states within the band gap (Fig. 8b).

The photocatalytic H_2 evolution reaction from aqueous methanol solution was took place before and after photodeposition of 1 wt% Pt onto titanates. Fig. 9 compares the H_2 evolution rate for unsubstituted tri- and tetratitanates. The pristine samples ($Na_2Ti_3O_7$ and $K_2Ti_3O_7$) showed very low activities; the H_2 evolution rate over $Na_2Ti_3O_7$ (0.15 mmol/h · g-cat) was two orders of magnitude less than that over a TiO_2 (anatase) photocatalyst (32 mmol/h · g-cat) under the same condition. The H_2 evolution rate was a little increased after protonation but decreased after SiO_2-pillaring. The apparent photocatalytic activity was enhanced by photodeposition of Pt. In particular, the most remarkable effect was observed when 1 wt.% Pt was deposited on the pillared samples. To evaluate their structure–activity relationship the microstructure of Pt-deposited samples was ob-

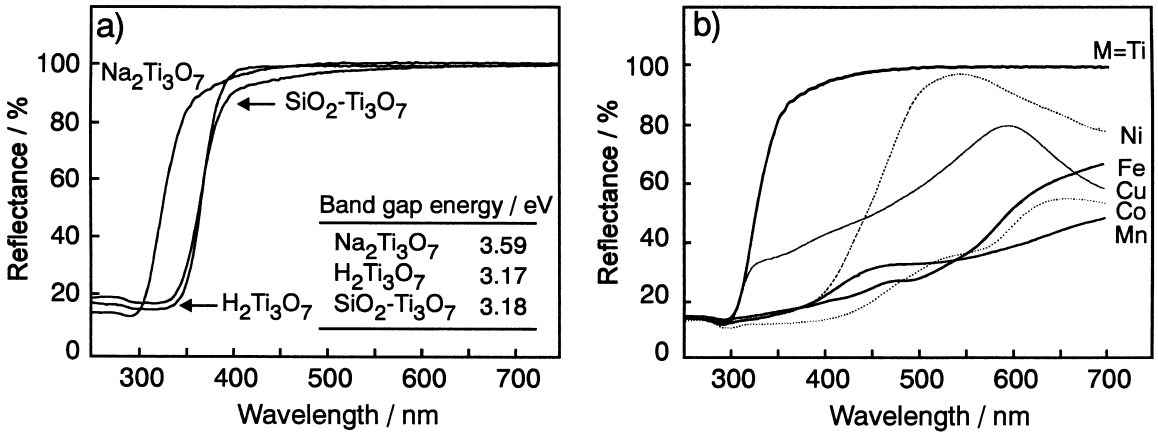

Fig. 8. UV–vis diffuse reflectance spectra of (a) trititanates after exchange and pillaring, and (b) $Na_2Ti_{3-x}M_xO_7$.

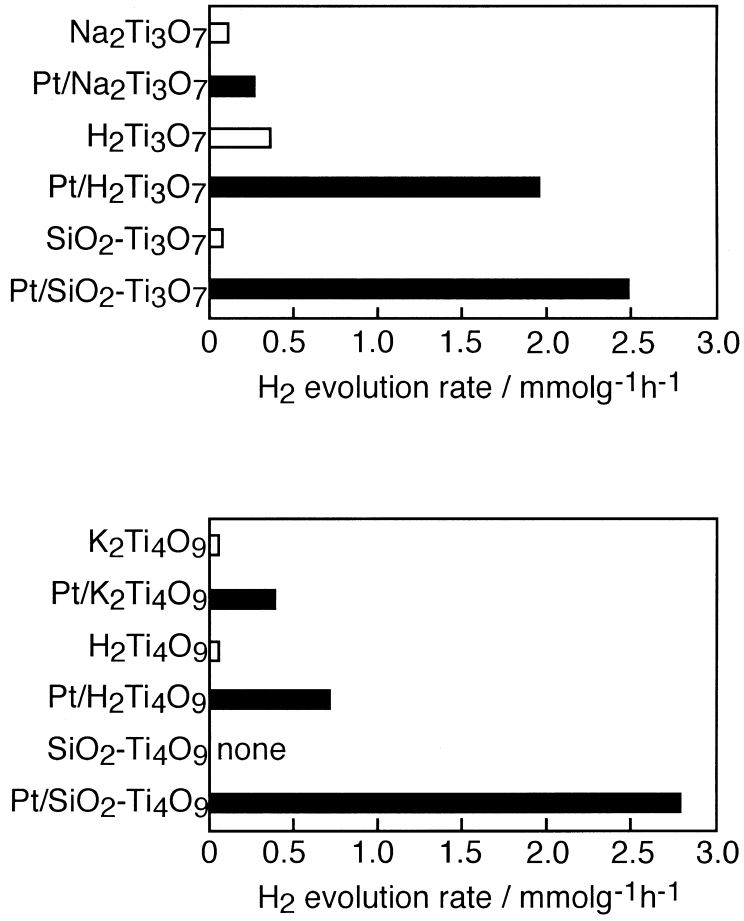

Fig. 9. Photocatalytic activity of layered tri- and tetratitanates for H_2 evolution. Pillared samples were calcined at 400°C. Loading of Pt is 1 wt.%.

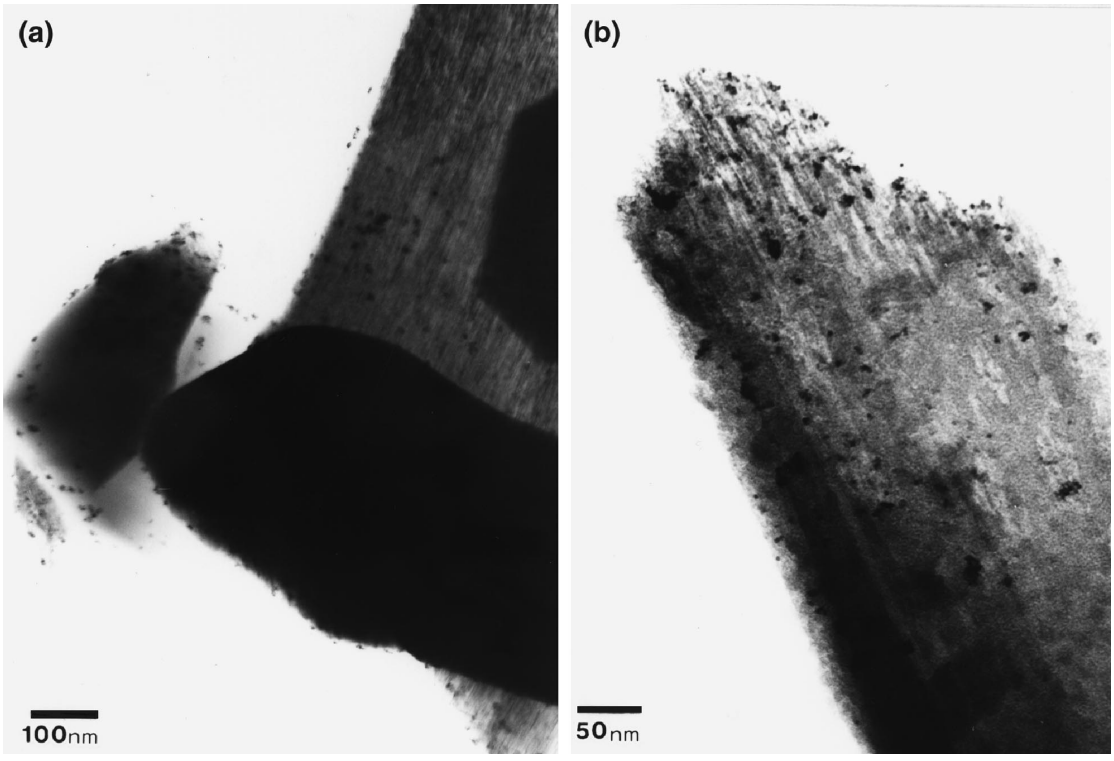

Fig. 10. TEM images of (a) $Na_2Ti_3O_7$ and (b) SiO_2-pillared trititanate after photodeposition of platinum.

served by using TEM (Fig. 10). Platinum was deposited as particles with several nm in diameter on the surface of unpillared microcrystals. On the SiO_2-pillared sample, however, Pt particles were deposited not only on the outer surface but also inside slit-like pores. Thus, the elevation of photocatalytic activity is associated with higher dispersion of Pt particles in the pillared pore structure. It was also reported by Domen et al. [10], the photocatalytic activity of platinized (0.1 wt.%) layered niobate, $KCa_2Nb_3O_{10}$, is enhanced by SiO_2 pillaring in accord with an increase of surface area. However, the present study has revealed that, without Pt loading, the SiO_2-pillared titanate is less active as compared to pristine or protonated sample. According to our preliminary XPS results, pillared samples contained SiO_2 on their outer surface due to adsorption of TEOS to the titanate surface in the pillaring process. The resultant surface impurity species may affect the charge transfer processes to bring about the H_2 evolution. Actually, it is known that a small amount of SiO_2 added to TiO_2 photocatalysts promotes recombination of photoexcited holes and electrons [13].

The effect of partial substitution on the catalytic activity of SiO_2-pillared trititanates is summarized in Fig. 11. The activity of unplatinized samples was little affected by the substitution up to $x = 0.15$, but drastically changed at $x = 0.3$. The resultant activity of SiO_2-pillared $Ti_{2.7}M_{0.3}O_7$ increased in a following sequence, $M = Ti < Ni < Cu < Fe < Mn$. Since this order is different from that of the surface area shown in Fig. 3, the incorporated transition elements are supposed to play a key role in the H_2 evolution reactions. It is well known that, in many cases, doping of impurity into TiO_2 produces recombination centers and thus decreases the photocatalytic activity. However, the present result suggested that a large amount of substitution is effective in improving the activity of layered titanates. Although the detail role of

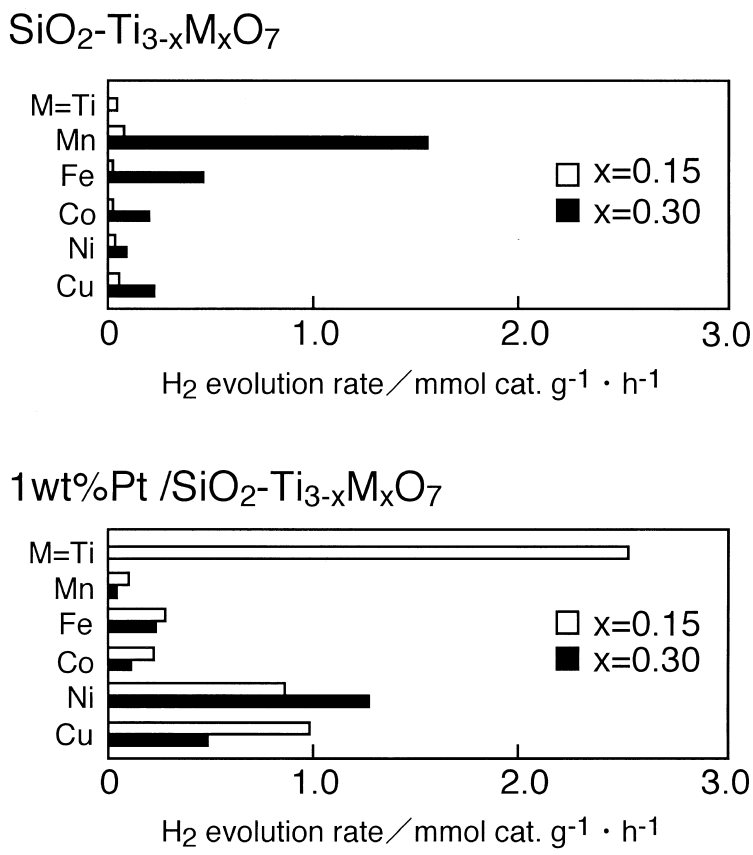

Fig. 11. Photocatalytic activity of SiO_2-pillared $Ti_{3-x}M_xO_7$ for H_2 evolution. Pillared samples were calcined at 400°C. Loading of Pt is 1 wt.%.

transition elements in photocatalysis has not been defined in the present stage, it seems relate to the change of photoabsorption property caused by the substitution. As was evident from UV–vis absorption spectra (Fig. 8), the substituted titanates showed absorption of visible light which may produce photoexcited species available for the H_2 evolution. However, there is another possible route for the improved activity, which is associated with the precipitation of transition metal oxides on the titanate surface. These impurity phases were invisible by XRD measurement, but small amount of transition metal oxides such as NiO will bring about high activities comparable to Pt when deposited on the pore surface. To confirm this point, we have to reexamine the local structural analysis of substituted pillared samples.

We have also measured the H_2 evolution over the substituted pillared sample after deposition of platinum, but their activities were totally different from those of unplatinized catalysts (Fig. 11). In this case, Mn-substituted catalyst ($x = 0.3$) was significantly deactivated, whereas unsubstituted sample, SiO_2-pillared Ti_3O_7, which itself showed very low activity, attained the highest H_2 evolution rate among supported Pt catalysts. The deactivation of SiO_2-pillared $Ti_{2.7}Mn_{0.3}O_7$ was not related to the structural collapse, because the XRD pattern and the BET surface area of the pillared sample was not changed after deposition of Pt. One possible scheme is that two different active sites, Pt and transition metals, take part in H_2 evolution and reoxidation of thus produced H_2 competitively. The reverse reactions of this type are well known

for the photocatalytic decomposition of pure water, but to our knowledge, no report exist in the literature concerning reverse reactions in the presence of sacrificial agents, such as methanol. Clearly, more work is required to establish the exact mechanism of this phenomenon. The route for hydrogen evolution in this system and the role of substituted transition metals remain unknown. Photocatalytic measurement for H_2 and O_2 evolution reactions as well as detailed structural characterization of substituted pillared samples by means of analytical TEM and gas adsorption are in progress. Further work is also in progress to synthesize other systems based on layered oxide semiconductors pillared by photocatalytically active oxides, such as TiO_2 and Fe_2O_3.

Acknowledgements

One of the authors (M.M.) gratefully acknowledges financial support from Salt Science Research Foundation.

References

[1] I.V. Mitchell (Ed.), Pillared Layered Structures: Current Trends and Applications, Elsevier Applied Science, London, 1990.
[2] S. Cheng, T.C. Wang, Inorg. Chem. 28 (1989) 1283.
[3] M.W. Anderson, J. Klinowski, J. Am. Chem. Soc. 29 (1990) 3260.
[4] M.E. Landis, B.A. Aufdembrink, P. Chu, I.D. Johnson, G.W. Kirker, M.K. Rubin, J. Am. Chem. Soc. 113 (1991) 3189.
[5] W. Hou, Q. Yan, X. Fu, J. Chem. Soc. Chem. Commun. (1994) 1371.
[6] W. Hou, B. Peng, Q. Yan, X. Fu, G. Shi, J. Chem. Soc. Chem. Commun. (1994) 253.
[7] J. Kondo, S. Shibata, Y. Ebina, K. Domen, A. Tanaka, J. Phys. Chem. 99 (1995) 16043.
[8] W. Hou, Q. Yan, B. Peng, X. Fu, J. Mater. Chem. 5 (1995) 109.
[9] C. Guo, W. Hou, M. Guo, Q. Yan, Y. Chen, J. Chem. Soc. Chem. Commun. (1997) 801.
[10] K. Domen, Shokubai 34 (1992) 502.
[11] S. Uchida, Y. Yamamoto, Y. Fujishiro, A. Watanabe, O. Ito, T. Sato, J. Chem. Soc., Faraday Trans. 93 (1997) 3229.
[12] H. Izawa, S. Kikkawa, M. Koizumi, J. Phys. Chem. 86 (1982) 5023.
[13] M. Anpo, T. Shima, S. Kodama, Y. Kubokawa, J. Phys. Chem. 91 (1987) 4305.